

CLIP-Count: Towards Text-Guided Zero-Shot Object Counting

Ruixiang Jiang
rui-x.jiang@connect.polyu.hk
The Hong Kong Polytechnic
University
HKSAR, China

Lingbo Liu
lingbo.liu@polyu.edu.hk
The Hong Kong Polytechnic
University
HKSAR, China

Changwen Chen*
changwen.chen@polyu.edu.hk
The Hong Kong Polytechnic
University
HKSAR, China

ABSTRACT

Recent advances in visual-language models have shown remarkable zero-shot text-image matching ability that is transferable to downstream tasks such as object detection and segmentation. Adapting these models for object counting, however, remains a formidable challenge. In this study, we first investigate transferring vision-language models (VLMs) for class-agnostic object counting. Specifically, we propose **CLIP-Count**, the first end-to-end pipeline that estimates density maps for open-vocabulary objects with text guidance in a zero-shot manner. To align the text embedding with dense visual features, we introduce a patch-text contrastive loss that guides the model to learn informative patch-level visual representations for dense prediction. Moreover, we design a hierarchical patch-text interaction module to propagate semantic information across different resolution levels of visual features. Benefiting from the full exploitation of the rich image-text alignment knowledge of pretrained VLMs, our method effectively generates high-quality density maps for objects-of-interest. Extensive experiments on FSC-147, CARPK, and ShanghaiTech crowd counting datasets demonstrate state-of-the-art accuracy and generalizability of the proposed method. Code is available: <https://github.com/songrise/CLIP-Count>.

CCS CONCEPTS

• Computing methodologies → Computer vision tasks.

KEYWORDS

class-agnostic object counting, clip, zero-shot, text-guided

ACM Reference Format:

Ruixiang Jiang, Lingbo Liu, and Changwen Chen. 2023. CLIP-Count: Towards Text-Guided Zero-Shot Object Counting. In *Proceedings of the 31st ACM International Conference on Multimedia (MM '23)*, October 29–November 3, 2023, Ottawa, ON, Canada. ACM, New York, NY, USA, 12 pages. <https://doi.org/10.1145/3581783.3611789>

1 INTRODUCTION

Over the past decade, object-specific (*e.g.*, crowd and vehicle) counting has been extensively studied [5, 11, 20–23, 29, 36, 40, 44, 46].

*Changwen Chen is the corresponding author. This research is supported by The Hong Kong Polytechnic University (ZVVK-P0036744).

Permission to make digital or hard copies of all or part of this work for personal or classroom use is granted without fee provided that copies are not made or distributed for profit or commercial advantage and that copies bear this notice and the full citation on the first page. Copyrights for components of this work owned by others than the author(s) must be honored. Abstracting with credit is permitted. To copy otherwise, or republish, to post on servers or to redistribute to lists, requires prior specific permission and/or a fee. Request permissions from [permissions@acm.org](https://permissions.acm.org).

MM '23, October 29–November 3, 2023, Ottawa, ON, Canada

© 2023 Copyright held by the owner/author(s). Publication rights licensed to ACM.

ACM ISBN 979-8-4007-0108-5/23/10...\$15.00

<https://doi.org/10.1145/3581783.3611789>

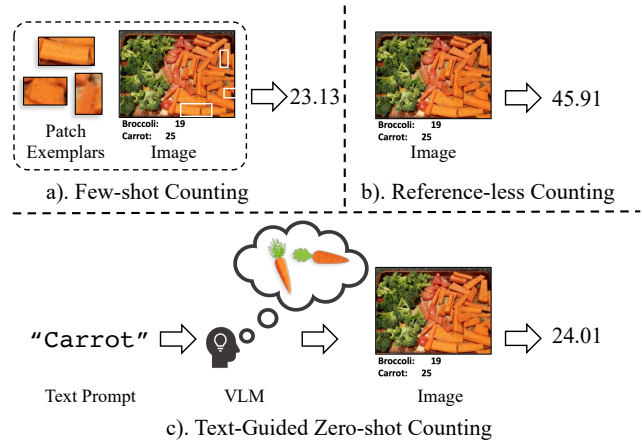


Figure 1: Illustration of different schemes of generalized object counting. a) Few-shot counting requires manually-labeled image patches for training and inference. b) Reference-less counting mines and counts salient objects automatically, but it cannot specify objects-of-interest. c) Zero-shot counting uses text prompts to specify and count objects of interest via pretrained VLM, without relying on manual annotations.

Despite the progress, it requires training a specific network with massively labeled samples for each class of objects. In contrast, human counting ability is agnostic to specific object classes. When presented with previously unseen objects, we identify, compare, and treat similar objects as the counting target [2]. This observation has motivated the emergence of class-agnostic object counting algorithms [3, 6, 16, 19, 25, 31, 38, 41, 50], which aim at training a unified/shared model to estimate the number of arbitrary objects-of-interest in the given image, as shown in Fig. 1-(a). By annotating a few image patches as exemplars and computing the similarities between exemplars and image regions, these methods have achieved good generalizability and counting accuracy.

However, most previous class-agnostic counting methods assume that accurate bounding boxes of exemplars are easily available both during training and inference, which is not always the case in real-world applications. Therefore, in practice, they usually request users to manually annotate the exemplars of objects-of-interest, which is unfriendly to end-users. Moreover, even when exemplars are annotated, the high intra-class variance of query objects can still lead to biased object counts [19, 41]. To address these issues, reference-less counting methods have been proposed to automatically mine and count salient objects at inference time [6, 31]. While

these approaches avoid cumbersome manual annotation, they lack the discriminative ability to specify the object class of interest in the presence of multiple object classes, as illustrated in Fig. 1-(b). Overall, the limitations of existing counting schemes highlight the need for more flexible and robust guidance in generalized object counting.

In this work, we challenge the conventional notion that self-similarity between exemplars and the query image is essential for generalized object counting. To this end, we propose a new counting scheme called text-guided zero-shot object counting, which utilizes an additional natural language prompt as input to query object count in given images, as shown in Fig. 1-(c). In particular, the use of text prompts as guidance offers two main benefits. Firstly, it reduces the need for manual annotation of patch exemplars both during training and testing, making it more user-friendly and scalable to larger datasets. Secondly, text prompts offer greater flexibility compared to patch exemplars, as they can cover both general descriptions such as "food" and specific descriptions such as "red apple in a basket". Therefore, our text-guided scheme is more flexible and promising for class-agnostic object counting.

However, using natural language to guide generalized object counting presents several challenges. Firstly, unlike patch annotations that provide explicit appearance and shape information, text prompts only contain implicit descriptions of the query object, which can be intrinsically ambiguous. Additionally, text prompts are expected to precisely locate objects-of-interest in input images, and the effective semantic alignment of these two modalities is non-trivial. Moreover, achieving zero-shot object counting requires the model to be generalizable to open-vocabulary text prompts and object classes, but the lack of large-scale annotated datasets severely hinders the development and evaluation of text-guided zero-shot object counting methods.

Taking the above issues into consideration, we propose a unified text-guided zero-shot object counting method, termed **CLIP-Count**. Specifically, our method is developed based on Contrastive Language-Image Pre-training [30] (CLIP), which endows our model with zero-shot image-text alignment ability. To transfer the powerful image-level CLIP to dense tasks such as density estimation, we first design a patch-text contrastive loss to align text and patch embedding space. This alignment is achieved by simultaneously tuning visual [10] and text prompts [49, 50] to enable parameter-and-data-efficient transfer learning of pretrained CLIP. To propagate textual information to dense image features for text-guided counting, we further elaborate a hierarchical patch-text interaction module that correlates text and image to different resolutions. Thanks to those tailor-designed modules, our method can effectively exploit the rich image-text alignment knowledge of CLIP to generate high-quality density maps for objects-of-interest. Extensive experiments on FSC-147 [32], CARPK [8], and ShanghaiTech crowd counting [47] dataset demonstrate that our method is effective and generalizable to unseen object classes and text prompts.

In summary, our major contributions are as follows:

- To the best of our knowledge, our CLIP-Count is the first end-to-end text-guided zero-shot object counting model, which is flexible and scalable in real-world applications.
- We propose a novel approach whereby visual prompts and text prompts are learned simultaneously to fully exploit the rich pre-trained knowledge of CLIP.
- We propose two tailored modules (*i.e.*, patch-text contrastive loss and hierarchical patch-text interaction module) to improve the counting ability of CLIP.
- Extensive experiments conducted on three object counting datasets demonstrate the state-of-the-art accuracy and generalizability of the proposed CLIP-Count method.

2 RELATED WORKS

2.1 Few-shot Object Counting

Few-shot object counting algorithms aim to learn a generalized model that counts anything with exemplar as inference-time guidance. The pioneering work, GMN [25] first formulates class-agnostic counting as a matching problem to exploit the self-similarity in counting tasks. Following this work, FamNet [32] learns to predict density maps with ROI pooling, and they further introduce a new dataset for class-agnostic counting, namely FSC-147 [32]. Subsequent advancements can be categorized into two streams. One approach involves utilizing more advanced visual backbones, such as vision transformers (ViT), to enhance the extracted feature representation (*e.g.*, CounTR [19], LOCA [3]). The second idea is to enhance the exemplar matching process by explicitly modeling exemplar-image similarity (*e.g.*, BMNet [35], SAFECOUNT [43]) or by further exploiting exemplar guidance [3, 18, 38]. Despite their good performance, all of those methods require additional patch-level annotation at training and inference time, which could be costly to obtain.

2.2 Reference-less and Zero-shot Object Counting

Reference-less counting has recently emerged as a more promising direction for class-agnostic counting without human annotation. The earliest attempt, RepRPN-Counter [31], proposes a region proposal module to extract the salient object in replacement of exemplar input. RCC [6] leverages pretrained ViT [1, 4] to implicitly extract the salient objects, and directly regress a scalar as the estimated object count. Notably, some recent few-shot counting models [3, 19, 38] could also be configured to perform reference-less counting. While those methods do not need exemplars, they fail to provide a way for specifying object-of-interest in presence of multiple object classes. Concurrent with this work, Xu *et al.* [41] introduces the task of zero-shot object counting, where only the class name is needed in inference time. They employ a two-stage training scheme: in the first stage, they train a few-shot object counter with exemplar supervision, and to achieve zero-shot counting, they additionally train a text-conditional variational autoencoder (VAE) on a closed-set of objects to generate exemplar prototypes. While their work shares similarities with ours at a high level, the key difference is that their two-stage training scheme still necessitates patch exemplars for training. In contrast, our method could be trained end-to-end without patch-level supervision.

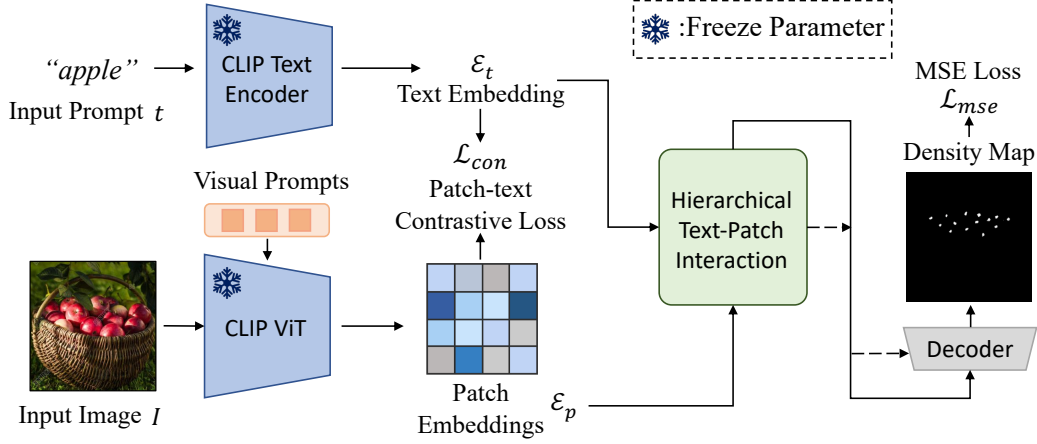


Figure 2: Overview of our CLIP-Count. We freeze both encoders in pretrained CLIP and append a small amount of learnable prompts to transfer the pretrained knowledge. A patch-text contrastive loss is employed to align dense visual features with text. To interact the two modalities, we design a hierarchical text-patch interaction module that outputs two multi-modal feature maps at different resolutions. Finally, we decode the multi-modal feature maps with a CNN decoder.

2.3 Vision-Language Pre-training

VLMs pre-trained on extremely large dataset demonstrate advanced zero-shot image-text matching ability [9, 12, 30]. In particular, CLIP [30] learns an aligned multi-modal embedding space, and it has inspired various applications that use it as an image-level classifier [7, 28, 37, 45]. To further exploit the powerful image-level representation in CLIP to perform dense tasks, DenseCLIP [33] elaborates a context-aware prompting technique to facilitate dense prediction such as segmentation. Concurrently, RegionCLIP [48] identifies the lack of localization ability issue in CLIP, and they distill pre-trained knowledge in CLIP to enable fine-grained image-region matching. More recently, ZegCLIP [51] designs a one-stage framework that calculate object masks based on patch embeddings for segmentation, while GridCLIP [17] aligns grid-level representation with text to enable one-stage object detection. The majority of those improvements focus on segmentation and detection. Very recently, two CLIP-based object counting models were proposed [15, 27], both based on image-level classification and limited in counting granularity and accuracy. Currently, it remains a challenge to achieve density estimation with VLMs.

3 METHOD

In this section, we present our proposed method, CLIP-Count, for text-guided zero-shot object counting. We will first review the structure of CLIP in Sec. 3.1. The objective of zero-shot class-agnostic object counting is defined in Sec. 3.2. We elaborate on the design of our proposed method in Sec. 3.3, and Sec. 3.4.

3.1 Preliminary: CLIP

CLIP [30] connects image and language through large scale pre-training on image and text pairs. It learns to align the text and image representations, so that the similarity of image and text pair could be calculated by dot product of their respective embeddings. Formally, let $\mathcal{E}_I \in \mathbb{R}_n$ and $\mathcal{E}_t \in \mathbb{R}_n$ denote the embedding of an image I and a text t , where $n = 512$ is the dimension of CLIP

embedding space. The cosine similarity of the text and image pair could be calculated as:

$$\text{CLIP}(I, t) = \frac{\mathcal{E}_t \cdot \mathcal{E}_I}{\|\mathcal{E}_t\| \|\mathcal{E}_I\|} \quad (1)$$

CLIP employs two encoders for encoding the image and text. Specifically, the last layer of ViT-based CLIP visual encoder [4] outputs a global image feature $z_0 \in \mathbb{R}_d$ and a 1/16 resolution patch-level feature map $z_x \in \mathbb{R}_{p^2 \times d}$, where $p = 14$ denotes the number of image patches per column and row, and $d = 768$ represents ViT latent dimension. CLIP applies a linear projection $\phi_z : \mathbb{R}_d \mapsto \mathbb{R}_n$ over the global feature to get the image embedding $\mathcal{E}_I = \phi_z(z_0)$, while the patch-level feature map z_x is discarded. In this work, we focus on utilizing z_x for density estimation.

3.2 Objective

Our objective is to count anything with text guidance. Formally, given an image $I \in \mathbb{R}_{H \times W \times 3}$ that contains arbitrary object class(es) as well as a natural language prompt t that specifies the object(s) of interest, our objective is to estimate a density map $\hat{y} \in \mathbb{R}_{H \times W}$ for the specified object(s). The estimated object count could be calculated by summing the density map $N_{pred} = \text{SUM}(\hat{y})$.

We denote the object classes contained in each set as $C_{train}, C_{val}, C_{test}$. Under the class-agnostic setting, the testing and validation sets do not overlap with the training set: $C_{train} \cap C_{val} = \emptyset$ and $C_{train} \cap C_{test} = \emptyset$. We optimize the model $F_\theta(I, t) = \hat{y}$ on the training set using ground truth density map supervision y , and evaluate its performance on the validation and testing sets.

It is worth noting that incorporating text guidance at inference time is a standard practice both for zero-shot object counting [41] and for other text-driven tasks with CLIP [7, 34, 37, 51]. Additionally, previous research [3, 6, 19] use the terms “reference-less counting” and “zero-shot counting” interchangeably, despite their inherent differences. For clarity, we refer to the methods that solely utilize image input as “reference-less”, while those that incorporate text as

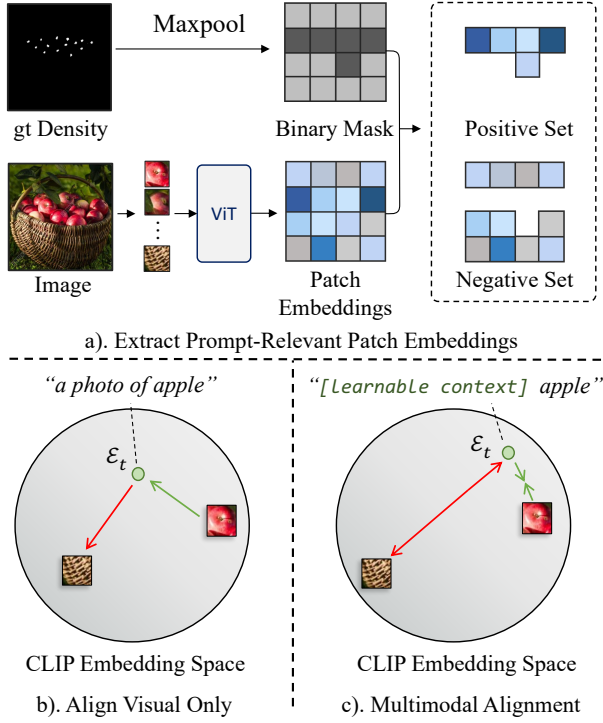


Figure 3: Illustration of patch-text contrastive loss. a.) we utilize g.t. density map to determine the objectness at patch-level, and we split the patch embeddings into two sets accordingly; b) finetune the visual encoder to align patch embeddings to the fixed text embedding space; c) shift both text and patch embeddings. The number of patches in a) and the two image patches in b) and c) are only for illustration purposes.

guidance are referred to as "zero-shot counting". Fig. 1 summarizes their difference.

3.3 Aligning Text with Dense Visual Features

CLIP has demonstrated remarkable performance in measuring global image-text similarity. However, transferring such ability to pixel level for dense-prediction is non-trivial, as the vanilla CLIP intrinsically lacks localization ability [14, 33], which limits its performance in object detection, segmentation, and counting. To alleviate this limitation, we propose adapting the CLIP vision encoder to enhance the localization ability of patch-level feature map z_x .

To be more specific, we propose a patch-text contrastive loss that maximizes the mutual information between text prompt and prompt-relevant patch-level features. To achieve this, we first apply a linear projection $\phi_p: \mathbb{R}_d \mapsto \mathbb{R}_n$ to map z_x to the same channel dimension as the text embedding \mathcal{E}_t :

$$\{\mathcal{E}_p^i = \phi_p(z_x^i) | i = 1, 2, \dots, p^2\} \quad (2)$$

For brevity, we call the reshaped $\mathcal{E}_p \in \mathbb{R}_{p \times p \times n}$ as *patch embeddings* of the input image. It is worth noting that this naming differs from the convention used in ViT, as our \mathcal{E}_p encodes cross-patch information due to the image-level perceptive field in global

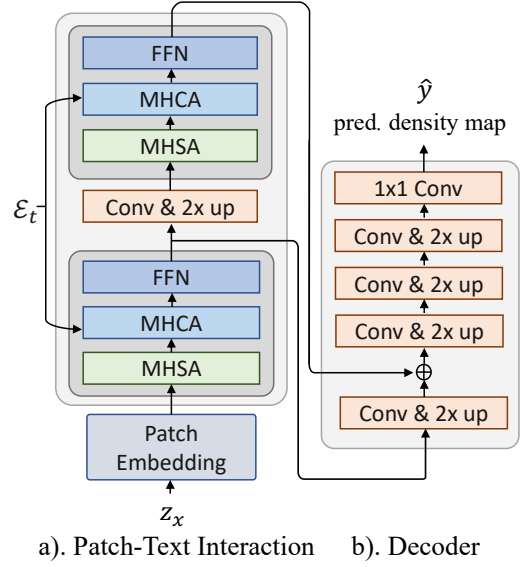


Figure 4: Architecture of the proposed hierarchical patch-text interaction module and the decoder. For brevity, we omit layer norms, positional encoding, and activation functions.

attention [4]. To determine the location of objects, we maxpool the ground truth density map y to get a patch-level binary mask $\mathcal{M} \in \mathbb{R}_{p \times p}$ for objectness. We then define \mathcal{P} and \mathcal{N} as the positive and negative sets of patch embeddings, depending on their corresponding mask value. Similar as [35, 39], we introduce the following InfoNCE-based [26] contrastive loss:

$$\mathcal{L}_{con} = -\log \frac{\sum_{i \in \mathcal{P}} \exp(s(\mathcal{E}_p^i, \mathcal{E}_t)/\tau)}{\sum_{i \in \mathcal{P}} \exp(s(\mathcal{E}_p^i, \mathcal{E}_t)/\tau) + \sum_{k \in \mathcal{N}} \exp(s(\mathcal{E}_p^k, \mathcal{E}_t)/\tau)} \quad (3)$$

where $s(\cdot, \cdot)$ denotes cosine similarity, and $\tau = 0.07$ is the temperature parameter [26]. The contrastive loss function in Eqn. 3 aligns the patch embedding space with the text embedding space by pulling positive patch embeddings closer to the fixed text embedding and pushing negative patches further away, which is analogous to the pre-training objective of CLIP [30]. Furthermore, we find it beneficial to adjust both the patch and text embeddings simultaneously, as the prompt templates used by CLIP such as "a photo of {class}" typically describe the image as a whole, rather than at the patch level. Inspired by CoOp [50], we optimize continuous token embeddings as the context of input prompt in an end-to-end manner. The entire procedure is summarized in Fig. 3.

3.4 Adapting CLIP for Density Estimation

Our patch-text contrastive loss aims to enhance the patch-level representation and improve the localization ability of CLIP. Nonetheless, two key questions remain: 1) How should the visual encoder be fine-tuned? and 2) How can the patch-level feature map be decoded into a text-conditional density map? In this section, we will address these questions.

Visual Prompt Tuning. Our model involves transferring the pretrained knowledge in CLIP visual transformer for dense prediction. However, the conventional “*pre-training + finetuning*” paradigm would be computationally expensive as it requires updating the entire model. Furthermore, finetuning a transformer usually requires a significant amount of data, which may not be practical when annotations are expensive to obtain, as is often the case with object counting. To effectively exploit the pretrained knowledge in CLIP, we instead freeze the parameters in CLIP ViT, and concatenate a small amount of trainable parameters as visual prompts [10] to the input of each transformer layer. This allows us to transfer the knowledge in CLIP using a much smaller amount of data and memory while still benefiting from the rich visual representation learned in CLIP. We refer readers to the original paper on visual prompt tuning (VPT) [10] for further details.

Hierarchical Text-Patch Interaction Module. Objects in a scene usually span a variety of scales, yet the homogenous transformer structure intrinsically lacks the inductive bias for modeling scale-invariant features [13], resulting in inaccurate density estimation. To address this issue, we propose a lightweight hierarchical transformer with cross-attention to enable the propagation of text information to different scales of the image feature. Our interaction module comprises two similar blocks, where each block sequentially applies multihead self-attention (MHSA), multihead cross-attention (MHCA), and a two-layer MLP (FFN). The MHSA captures long-distance relationships, while the MHCA propagates semantic information embedded in text to visual features. In between the two layers, a convolution layer with a skip connection is employed, followed by a $2\times$ bi-linear interpolation layer that doubles the resolution of the intermediate multi-modal feature map $M_c \in \mathbb{R}_{p \times p \times n}$. The motivation is to capture the relationship between text and image at a finer granularity [13]. The final output of the interaction module are the coarse M_c and fine $M_f \in \mathbb{R}_{2p \times 2p \times n}$ multi-modal feature maps. As validated in the Appendix, we find the two-scale design provides the best balance between cost and accuracy. The entire interaction process is visualized in Fig. 4-(a).

Density Map Regression. We decode the multi-modal feature maps $\{M_c, M_f\}$ using a CNN-based decoder, as illustrated in Fig. 4-(b). The decoder consists of several convolutional layers and $2\times$ interpolation layers that sequentially doubles the spatial resolution and decrease the channel dimension by half. To decode the two-scale feature maps from the interaction module, we first perform convolution on the coarse multi-modal map M_c , and fuse it with M_f before the second convolution by summation:

$$M'_f = \text{Lerp}(\sigma(\text{Conv}_{3 \times 3}(M_c))) + \sigma(\text{Conv}_{1 \times 1}(M_f)) \quad (4)$$

where $\text{Lerp}(\cdot)$ denotes bi-linear interpolation, $\sigma(\cdot)$ is the activation function. The final output of the decoder \hat{y} is obtained through a 1×1 convolution layer with sigmoid activation.

4 EXPERIMENTS

4.1 Dataset

FSC-147. FSC-147 [32] is a dataset recently proposed for class-agnostic object counting. It consists of 6,135 images across 147 object classes, with non-overlapping object classes in each set. For

each training image, the dataset provides its class name, dot supervision, and three random bounding boxes of objects (*i.e.*, the exemplar patch annotation). In our experiments, we use the class name as the text prompt t , and we do not use the patch annotation.

CARPK. CARPK [8] provides 1448 birds-eye view image of parking lots, containing a total of 89,777 cars. We use CARPK to evaluate the cross-dataset transferability of CLIP-Count.

ShanghaiTech. The ShanghaiTech crowd counting dataset [47] is a comprehensive dataset for crowd counting. It comprises two parts, A and B, with a total of 1,198 annotated images. Part A consists of 482 images, with 400 designated for training and 182 for testing. Part B comprises 716 images, with 400 for training and 316 for testing. Notably, the two parts were collected using different methods, which presents a challenge for cross-part evaluation.

4.2 Implementation Details

Architecture Detail. We use OpenAI pre-trained CLIP with ViT-B/16 backbone. For the visual encoder, we use the deep version of VPT, with 20 visual prompts in each layer. For context learning, we use 2 prefix tokens. The maxpooling in contrastive loss adopts a kernel size of 16×16 and stride = 16, no padding is used. For the density decoder, we use 3×3 convolution kernel with stride = 1 and padding = 1 to keep spatial resolution. GeLU non-linearity is used after each convolution layers.

Training Detail. The model is trained on the training set of FSC-147. We view our proposed contrastive loss as a pretext task to improve feature representation. Therefore, we first pre-train the model with contrastive loss only for 30 epochs before further train it with mean square error (MSE) loss for 200 epochs. The MSE loss is defined as $\mathcal{L}_{MSE} = \|y - \hat{y}\|^2 / (H \times W)$.

During both training stages, we use a batch size of 32, and use AdamW [24] optimizer with a learning rate of 1×10^{-4} , which decays by a factor of 0.33 after 100 epochs. The whole training process takes approximately 3 hours on a single Nvidia RTX-3090Ti GPU. We apply the same data augmentations as used in CounTR [19], except for their proposed mosaic augmentation. Additionally, to comply with the input assumption of CLIP, we downsample the training images to 224×224 , whereas previous generalized counting methods on FSC-147 typically use a resolution of 384×384 .

4.3 Evaluation Metrics

Following previous class agnostic counting methods [3, 6, 19, 32, 41], we evaluate the performance by mean absolute error (MAE) and root mean squared error (RMSE).

$$\text{MAE} = \frac{1}{N_I} \sum_{i=1}^{N_I} |N_{pred}^i - N_{gt}^i|, \text{RMSE} = \sqrt{\frac{1}{N_I} \sum_{i=1}^{N_I} (N_{pred}^i - N_{gt}^i)^2} \quad (5)$$

where N_I denotes the number of images in testing set, and N_{pred} , N_{gt} is the predicted and ground truth object count.

5 RESULT AND ANALYSIS

5.1 Quantitative Result

To the best of our knowledge, this is the first investigation into the application of VLMs for zero-shot density map regression in

Table 1: Comparison with state-of-the-art methods on FSC-147. (*) denotes adopting modification for reference-less counting as described in RCC [6]. We highlight the best result for each scheme in bold.

Scheme	Method	Source	#Shot	Val Set		Test Set	
				MAE	RMSE	MAE	RMSE
Few-shot	FamNet [32]	CVPR2021	3	24.32	70.94	22.56	101.54
	CFOCNet [42]	WACV2021	3	21.19	61.41	22.10	112.71
	CounTR [19]	BMVC2022	3	13.13	49.83	11.95	91.23
	LOCA [3]	arXiv2022	3	10.24	32.56	10.97	56.97
	FamNet [32]	CVPR2021	1	26.05	77.01	26.76	110.95
Reference-less	FamNet* [32]	CVPR2021	0	32.15	98.75	32.27	131.46
	RepRPN-C [31]	ACCV2022	0	29.24	98.11	26.66	129.11
	CounTR [19]	BMVC2022	0	18.07	71.84	14.71	106.87
	LOCA [3]	arXiv2022	0	17.43	54.96	16.22	103.96
	RCC [6]	arXiv2022	0	17.49	58.81	17.12	104.53
Zero-shot	Xu <i>et al.</i> [41]	CVPR2023	0	26.93	88.63	22.09	115.17
	Ours	MM2023	0	18.79	61.18	17.78	106.62

Table 2: Cross-dataset evaluation on CARPK dataset. (†) Trained using same backbone with ours.

Method	#Shot	MAE	RMSE
FamNet [32]	3	28.84	44.47
BMNet [35]	3	14.41	24.60
BMNet+ [35]	3	10.44	13.77
RCC [†] [6]	0	21.38	26.15
Ours	0	11.96	16.61

both the generalized counting and class-specific counting settings. Therefore, a direct comparison with previous methods is impractical. To evaluate the performance of our approach, we compare it to several state-of-the-art few-shot and reference-less generalized object counting methods, including FamNet [32], CFOCNet [42], CounTR [19], LOCA [3], RepRPN-C [31], RCC [6], and the only other zero-shot counting method [41] on FSC-147. Additionally, we compare our model with class-specific counting models on the CARPK and ShanghaiTech crowd counting datasets in a cross-dataset setting.

Quantitative Result on FSC-147. We compare CLIP-Count with state-of-the-art generalized counting methods on FSC-147, and summarize quantitative result in Tab. 1. Overall, we outperform the state-of-the-art zero-shot object counting method [41] on the FSC-147 dataset by a significant margin. We also compare our results with few-shot and reference-less methods for reference. Notice that zero-shot object counting aims to solve a more challenging scenario, as the model needs to understand the correspondence between text and visual features.

Quantitative Result on CARPK. Following previous class-agnostic counting methods [6, 25, 35], we test CLIP-Count on CARPK to evaluate its cross-dataset generalizability. Specifically, the model is trained on FSC-147 and evaluated on the testing set of CARPK without fine-tuning. To ensure fair comparison, we train

Table 3: Cross-dataset evaluation on ShanghaiTech crowd counting dataset. (†) Trained using same backbone with ours.

Method	Type	Training→Testing	MAE	RMSE
MCNN [47]	Specific	Part A→Part B	85.2	142.3
CrowdCLIP [15]		Part A→Part B	69.6	80.7
RCC [†] [6]	Generic	FSC147→Part B	66.6	104.8
Ours		FSC147→Part B	45.7	77.4
MCNN [47]	Specific	Part B→Part A	221.4	357.8
CrowdCLIP [15]		Part B→Part A	217.0	322.7
RCC [†] [6]	Generic	FSC147→Part A	240.1	366.9
Ours		FSC147→Part A	192.6	308.4

RCC with the same visual backbone (i.e., Vit-B/16) on FSC-147, instead of their proposed FSC-133. As shown in Tab. 2, our approach outperforms the representative reference-less counting method, RCC, by a significant margin.

Quantitative Result on ShanghaiTech Crowd Counting. Concurrent with this work, Liang *et al.* [15] propose the first CLIP-based crowd counting method, namely CrowdCLIP. In their paper, they evaluate the cross-dataset performance of models by training the class-specific models on one part of the ShanghaiTech dataset and test on another. We conduct a similar experiment by directly evaluating our model and RCC [6] for crowd counting (*i.e.*, no finetuning on any part of ShanghaiTech). Similar as the experiment on CARPK, we have also modified the backbone of RCC to ensure fairness. The results are summarized in Tab. 3. Our proposed generic counting method outperforms the representative class-specific counting methods MCNN [47] and CrowdCLIP [15] by a significant margin, even without training on any part of the crowd-counting dataset. In particular, we outperform CrowdCLIP by 11.2%, 4.0%, 34.3%, and 3.7% under cross-dataset setting. Moreover, our method significantly outperforms the other reference-less counting method, RCC [6]. Overall, the experiment demonstrate the advanced cross-dataset generalizability of CLIP-Count.

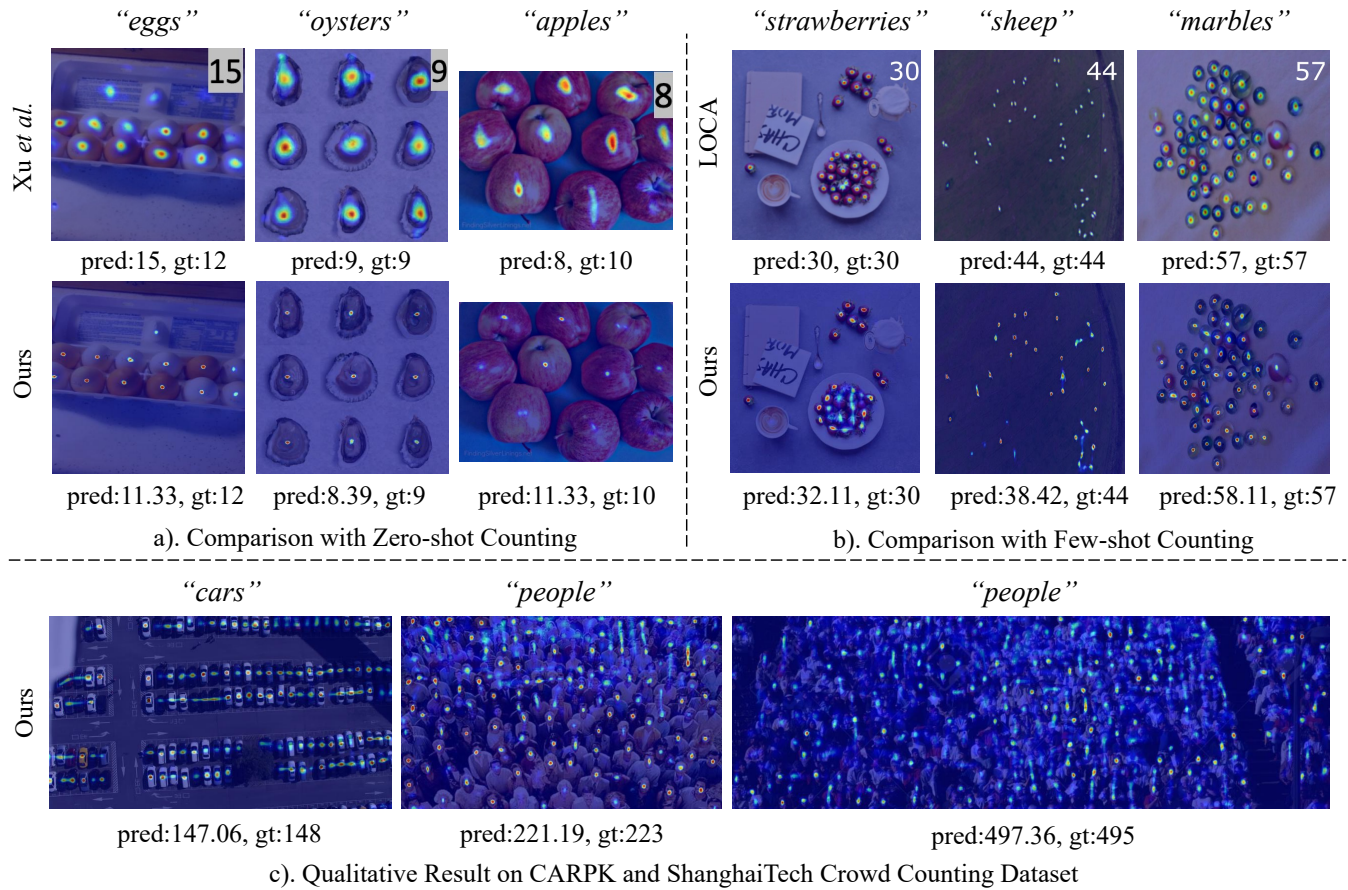


Figure 5: Qualitative result. We compare CLIP-Count with the state-of-the-art zero-shot [41] and few-shot counting method [3] on FSC-147 in a) and b), respectively. In c) we visualize results on the CARPK and ShanghaiTech crowd counting datasets.

Table 4: Ablate Study. We ablate (A) how to interact multi-modal feature; (B) how to transfer knowledge in CLIP; (C) how to apply contrastive loss. We show the number of trainable parameters and the evaluation metrics on the FSC-147 dataset.

Method	Interaction	Transfer	Contrastive	#Param.	Val Set		Test Set	
					MAE	RMSE	MAE	RMSE
A1	Add	Freeze	None	3.3M	30.40	96.67	33.84	124.64
A2	Naive	Freeze	None	16.0 M	32.50	95.02	31.48	121.95
A3	2-Scale	Freeze	None	16.6M	29.96	93.07	28.84	120.03
B1	Add	Finetune	None	89.4M	28.79	90.84	28.87	120.32
B2	2-Scale	Finetune	None	102.0M	24.88	77.73	22.51	131.12
B3	Add	VPT	None	4.0M	22.29	67.97	20.90	110.14
B4	Naive	VPT	None	16.6M	20.43	69.26	19.26	108.71
B5	2-Scale	VPT	None	17.3M	20.01	66.08	18.77	108.00
C1	2-Scale	VPT	Visual	17.3M	19.21	64.93	18.55	107.51
C2	2-Scale	VPT	Multi-modal	17.3M	18.79	61.18	17.78	106.62

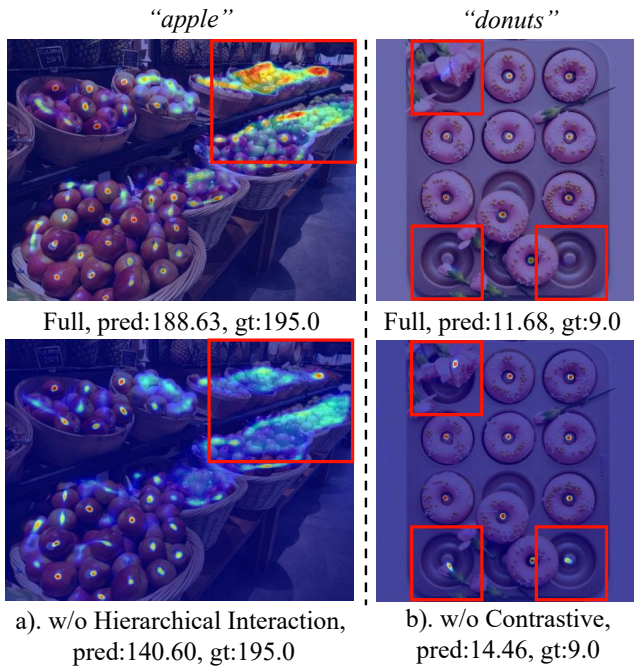


Figure 6: Visualization of ablation study. a.) Replace the hierarchical interaction with a plain transformer; b.) remove the contrastive loss.

5.2 Qualitative Result

We visualize qualitative results in Fig. 5, where we overlay the predicted density map on the input image. We provide a side-by-side comparison with our method against the state-of-the-art zero-shot counting method [41] in Fig. 5-(a), and few-shot method LOCA [3], in Fig. 5-(b) on the FSC-147 dataset from their paper. Compared with [41], our proposed method could better localize high density in the center of the object with high-fidelity. By contrast, the density prediction in [41] may exhibit non-concentrated patterns. Our model could also achieve competitive results with the representative few-shot counting method [3], both in terms of prediction error and fidelity of density maps. Additionally, we visualize results of crowded scenes from the CARPK and ShanghaiTech datasets in Fig. 5-(c). Overall, the proposed method robustly localizes and counts objects of different categories, shapes, sizes, and densities.

5.3 Ablation Study

We validate the design choices by iteratively adding components with different designs to our baseline model (A1). Specifically, we have ablated with the following three design choices: (A) how to interact text and image features from CLIP; (B) how to fine-tune CLIP ViT; and (C) the effect of patch-text contrastive loss. For (A), “*add*” means add text embedding to patch embeddings, “*naive*” means use a plain vision transformer [4, 19] without hierarchical design; for (B) “*finetune*” means finetune all ViT parameters; for (C) Contrastive loss, “*visual*” means adjust patch embeddings only, and “*multi-modal*” means adjust text and patch embeddings at the same

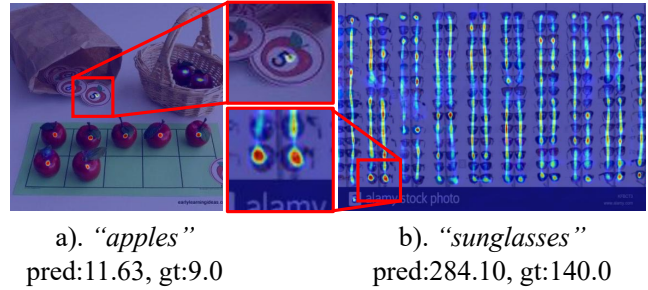


Figure 7: Representative failure cases due to a.) semantic ambiguity of the input prompt, b.) self-repeating structure of the queried object.

time. We summarize the results in Tab. 4, and we also visualize the effect of hierarchical interaction and contrastive loss in Fig. 6.

The proposed designs effectively improve the performance of our model. The cross-attention outperforms baseline (A1) in modeling complex text-image relationships. The hierarchical design of the interaction module further helps the model handle size variations of objects, such as the example in Fig. 6-(a). Additionally, the VPT enables parameter-and-data-efficient transfer learning, bringing 19.5% and 14.5% gains in MAE and RMSE (A3 vs. B5), respectively, with only 3% of additional parameters. The contrastive loss guides the model to align text and dense image features, resulting in improvements of 6.1% and 7.6% for both metrics (B5 vs. C2). Without the contrastive loss, the model may mistakenly treat visually similar objects as counting target, as exemplified in Fig. 6-(b).

5.4 Limitations and Future Works

CLIP-Count can be limited in certain scenarios due to ambiguity in text guidance for object counting. For example in Fig. 7-(a), the prompt “*apple*” can refer to either the fruit or a drawing of an apple, presenting a case of semantic ambiguity. When encounter linguistic ambiguity like this, our model may produce unwanted results. Another example is shown in Fig. 7-(b), where the queried object itself could be ambiguous, as the “*sunglasses*” consists of two similar lens, making it unclear whether they should be counted together or separately. We attribute these limitations to the inadequate prompt annotation in FSC-147, where only a general class name is available for text guidance. In future work, we plan to focus on collecting a dataset with more fine-grained text annotation to disambiguate the query object and enhance model accuracy.

6 CONCLUSION

In this paper, we show that pre-trained VLMs could be directly adopted for text-guided object counting tasks in an end-to-end manner. Specifically, we propose CLIP-Count, which fully exploits the pretrained knowledge in CLIP by aligning text embedding with patch-level visual features. Extensive experiments on the FSC-147, CARPK and ShanghaiTech crowd counting datasets demonstrate the state-of-the-art accuracy and generalizability of the proposed method for zero-shot object counting.

REFERENCES

- [1] Mathilde Caron, Hugo Touvron, Ishan Misra, Hervé Jégou, Julien Mairal, Piotr Bojanowski, and Armand Joulin. 2021. Emerging properties in self-supervised vision transformers. In *Proceedings of the IEEE/CVF international conference on computer vision*. 9650–9660.
- [2] Stanislas Dehaene. 2011. *The number sense: How the mind creates mathematics*. OUP USA.
- [3] Nikola Djukic, Alan Lukezic, Vitjan Zavrtanik, and Matej Kristan. 2022. A Low-Shot Object Counting Network With Iterative Prototype Adaptation. *arXiv preprint arXiv:2211.08217* (2022).
- [4] Alexey Dosovitskiy, Lucas Beyer, Alexander Kolesnikov, Dirk Weissenborn, Xiuhua Zhai, Thomas Unterthiner, Mostafa Dehghani, Matthias Minderer, Georg Heigold, Sylvain Gelly, et al. 2020. An image is worth 16x16 words: Transformers for image recognition at scale. *arXiv preprint arXiv:2010.11929* (2020).
- [5] Tao Han, Lei Bai, Junyu Gao, Qi Wang, and Wanli Ouyang. 2022. Dr. vic: Decomposition and reasoning for video individual counting. In *Proceedings of the IEEE/CVF Conference on Computer Vision and Pattern Recognition*. 3083–3092.
- [6] Michael Hobley and Victor Prisacariu. 2022. Learning to Count Anything: Reference-less Class-agnostic Counting with Weak Supervision. *arXiv preprint arXiv:2205.10203* (2022).
- [7] Fangzhou Hong, Mingyuan Zhang, Liang Pan, Zhongang Cai, Lei Yang, and Ziwei Liu. 2022. AvatarCLIP: Zero-Shot Text-Driven Generation and Animation of 3D Avatars. *arXiv preprint arXiv:2205.08535* (2022).
- [8] Meng-Ru Hsieh, Yen-Liang Lin, and Winston H Hsu. 2017. Drone-based object counting by spatially regularized regional proposal network. In *Proceedings of the IEEE international conference on computer vision*. 4145–4153.
- [9] Chao Jia, Yinfei Yang, Ye Xia, Yi-Ting Chen, Zarana Parekh, Hieu Pham, Quoc Le, Yun-Hsuan Sung, Zhen Li, and Tom Duerig. 2021. Scaling up visual and vision-language representation learning with noisy text supervision. In *International Conference on Machine Learning*. PMLR, 4904–4916.
- [10] Menglin Jia, Luming Tang, Bor-Chun Chen, Claire Cardie, Serge Belongie, Bharath Hariharan, and Ser-Nam Lim. 2022. Visual prompt tuning. *arXiv preprint arXiv:2203.12119* (2022).
- [11] Haopeng Li, Lingbo Liu, Kunlin Yang, Shinan Liu, Junyu Gao, Bin Zhao, Rui Zhang, and Jun Hou. 2022. Video Crowd Localization With Multifocus Gaussian Neighborhood Attention and a Large-Scale Benchmark. *IEEE Transactions on Image Processing* 31 (2022), 6032–6047.
- [12] Junnan Li, Dongxu Li, Caiming Xiong, and Steven Hoi. 2022. Blip: Bootstrapping language-image pre-training for unified vision-language understanding and generation. In *International Conference on Machine Learning*. PMLR, 12888–12900.
- [13] Yanghao Li, Hanzi Mao, Ross Girshick, and Kaiming He. 2022. Exploring plain vision transformer backbones for object detection. In *Computer Vision—ECCV 2022: 17th European Conference, Tel Aviv, Israel, October 23–27, 2022, Proceedings, Part IX*. Springer, 280–296.
- [14] Yi Li, Hualiang Wang, Yiqun Duan, and Xiaomeng Li. 2023. Clip surgery for better explainability with enhancement in open-vocabulary tasks. *arXiv preprint arXiv:2304.05653* (2023).
- [15] Dingkan Liang, Jiahao Xie, Zhikang Zou, Xiaoqing Ye, Wei Xu, and Xiang Bai. 2023. CrowdCLIP: Unsupervised Crowd Counting via Vision-Language Model. *arXiv preprint arXiv:2304.04231* (2023).
- [16] Hui Lin, Xiaopeng Hong, and Yabin Wang. 2021. Object Counting: You Only Need to Look at One. *arXiv preprint arXiv:2112.05993* (2021).
- [17] Jiayi Lin and Shaogang Gong. 2023. GridCLIP: One-Stage Object Detection by Grid-Level CLIP Representation Learning. *arXiv preprint arXiv:2303.09252* (2023).
- [18] Wei Lin, Kunlin Yang, Xinzhu Ma, Junyu Gao, Lingbo Liu, Shinan Liu, Jun Hou, Shuai Yi, and Antoni B Chan. 2022. Scale-Prior Deformable Convolution for Exemplar-Guided Class-Agnostic Counting. (2022).
- [19] Chang Liu, Yujie Zhong, Andrew Zisserman, and Weidi Xie. 2022. Countr: Transformer-based generalised visual counting. *arXiv preprint arXiv:2208.13721* (2022).
- [20] Lingbo Liu, Jiaqi Chen, Hefeng Wu, Tianshui Chen, Guanbin Li, and Liang Lin. 2020. Efficient crowd counting via structured knowledge transfer. In *Proceedings of the 28th ACM international conference on multimedia*. 2645–2654.
- [21] Lingbo Liu, Jiaqi Chen, Hefeng Wu, Guanbin Li, Chenglong Li, and Liang Lin. 2021. Cross-modal collaborative representation learning and a large-scale rgbt benchmark for crowd counting. In *Proceedings of the IEEE/CVF conference on computer vision and pattern recognition*. 4823–4833.
- [22] Lingbo Liu, Zhilin Qiu, Guanbin Li, Shufan Liu, Wanli Ouyang, and Liang Lin. 2019. Crowd counting with deep structured scale integration network. In *Proceedings of the IEEE/CVF international conference on computer vision*. 1774–1783.
- [23] Lingbo Liu, Hongjun Wang, Guanbin Li, Wanli Ouyang, and Liang Lin. 2018. Crowd counting using deep recurrent spatial-aware network. In *Proceedings of the 27th International Joint Conference on Artificial Intelligence*. 849–855.
- [24] Ilya Loshchilov and Frank Hutter. 2017. Decoupled weight decay regularization. *arXiv preprint arXiv:1711.05101* (2017).
- [25] Erika Lu, Weidi Xie, and Andrew Zisserman. 2018. Class-agnostic counting. In *Asian conference on computer vision*. Springer, 669–684.
- [26] Aaron van den Oord, Yazhe Li, and Oriol Vinyals. 2018. Representation learning with contrastive predictive coding. *arXiv preprint arXiv:1807.03748* (2018).
- [27] Roni Passa, Ariel Ephrat, Omer Tov, Shiran Zada, Inbar Mosseri, Michal Irani, and Tali Dekel. 2023. Teaching CLIP to Count to Ten. *arXiv preprint arXiv:2302.12066* (2023).
- [28] Or Patashnik, Zongze Wu, Eli Shechtman, Daniel Cohen-Or, and Dani Lischinski. 2021. Styleclip: Text-driven manipulation of stylegan imagery. In *Proceedings of the IEEE/CVF International Conference on Computer Vision*. 2085–2094.
- [29] Zhilin Qiu, Lingbo Liu, Guanbin Li, Qing Wang, Nong Xiao, and Liang Lin. 2019. Crowd counting via multi-view scale aggregation networks. In *2019 IEEE International Conference on Multimedia and Expo (ICME)*. IEEE, 1498–1503.
- [30] Alec Radford, Jong Wook Kim, Chris Hallacy, Aditya Ramesh, Gabriel Goh, Sandhini Agarwal, Girish Sastry, Amanda Askell, Pamela Mishkin, Jack Clark, et al. 2021. Learning transferable visual models from natural language supervision. In *International Conference on Machine Learning*. PMLR, 8748–8763.
- [31] Viresh Ranjan and Minh Hoai Nguyen. 2022. Exemplar free class agnostic counting. In *Proceedings of the Asian Conference on Computer Vision*. 3121–3137.
- [32] Viresh Ranjan, Udbhav Sharma, Thu Nguyen, and Minh Hoai. 2021. Learning to count everything. In *Proceedings of the IEEE/CVF Conference on Computer Vision and Pattern Recognition*. 3394–3403.
- [33] Yongming Rao, Wenliang Zhao, Guangyi Chen, Yansong Tang, Zheng Zhu, Guan Huang, Jie Zhou, and Jiwen Lu. 2022. Denseclip: Language-guided dense prediction with context-aware prompting. In *Proceedings of the IEEE/CVF Conference on Computer Vision and Pattern Recognition*. 18082–18091.
- [34] Aditya Sanghi, Hang Chu, Joseph G Lambourne, Ye Wang, Chin-Yi Cheng, Marco Fumero, and Kamal Rahimi Malekshah. 2022. Clip-forge: Towards zero-shot text-to-shape generation. In *Proceedings of the IEEE/CVF Conference on Computer Vision and Pattern Recognition*. 18603–18613.
- [35] Min Shi, Hao Lu, Chen Feng, Chengxin Liu, and Zhiguo Cao. 2022. Represent, Compare, and Learn: A Similarity-Aware Framework for Class-Agnostic Counting. In *Proceedings of the IEEE/CVF Conference on Computer Vision and Pattern Recognition*. 9529–9538.
- [36] Vishwanath A Sindagi and Vishal M Patel. 2017. Generating high-quality crowd density maps using contextual pyramid cnns. In *Proceedings of the IEEE international conference on computer vision*. 1861–1870.
- [37] Can Wang, Ruixiang Jiang, Menglei Chai, Mingming He, Dongdong Chen, and Jing Liao. 2022. NeRF-Art: Text-Driven Neural Radiance Fields Stylization. *arXiv preprint arXiv:2212.08070* (2022).
- [38] Mingjie Wang, Yande Li, Jun Zhou, Graham W Taylor, and Minglun Gong. 2023. GCNet: Probing Self-Similarity Learning for Generalized Counting Network. *arXiv preprint arXiv:2302.05132* (2023).
- [39] Zhaoping Wang, Yu Lu, Qiang Li, Xunqiang Tao, Yandong Guo, Mingming Gong, and Tongliang Liu. 2022. Cris: Clip-driven referring image segmentation. In *Proceedings of the IEEE/CVF conference on computer vision and pattern recognition*. 11686–11695.
- [40] Zhengtao Wu, Lingbo Liu, Yang Zhang, Mingzhi Mao, Liang Lin, and Guanbin Li. 2022. Multimodal Crowd Counting with Mutual Attention Transformers. In *IEEE International Conference on Multimedia and Expo*. IEEE, 1–6.
- [41] Jingyi Xu, Hieu Le, Vu Nguyen, Viresh Ranjan, and Dimitris Samaras. 2023. Zero-shot Object Counting. *arXiv preprint arXiv:2303.02001* (2023).
- [42] Shuo-Diao Yang, Hung-Ting Su, Winston H Hsu, and Wen-Chin Chen. 2021. Class-agnostic few-shot object counting. In *Proceedings of the IEEE/CVF Winter Conference on Applications of Computer Vision*. 870–878.
- [43] Zhiyuan You, Kai Yang, Wenhan Luo, Xin Lu, Lei Cui, and Xinyi Le. 2023. Few-shot object counting with similarity-aware feature enhancement. In *Proceedings of the IEEE/CVF Winter Conference on Applications of Computer Vision*. 6315–6324.
- [44] Lixian Yuan, Zhilin Qiu, Lingbo Liu, Hefeng Wu, Tianshui Chen, Pei Chen, and Liang Lin. 2020. Crowd counting via scale-communicative aggregation networks. *Neurocomputing* 409 (2020), 420–430.
- [45] Renrui Zhang, Ziyu Guo, Wei Zhang, Kunchang Li, Xupeng Miao, Bin Cui, Yu Qiao, Peng Gao, and Hongsheng Li. 2022. Pointclip: Point cloud understanding by clip. In *Proceedings of the IEEE/CVF Conference on Computer Vision and Pattern Recognition*. 8552–8562.
- [46] Shanghang Zhang, Guanhang Wu, Joao P Costeira, and José MF Moura. 2017. Fcn-rlstm: Deep spatio-temporal neural networks for vehicle counting in city cameras. In *Proceedings of the IEEE international conference on computer vision*. 3667–3676.
- [47] Yingying Zhang, Desen Zhou, Siqin Chen, Shenghua Gao, and Yi Ma. 2016. Single-image crowd counting via multi-column convolutional neural network. In *Proceedings of the IEEE conference on computer vision and pattern recognition*. 589–597.
- [48] Yiwu Zhong, Jianwei Yang, Pengchuan Zhang, Chunyuan Li, Noel Codella, Liunan Harold Li, Luwei Zhou, Xiyang Dai, Lu Yuan, Yin Li, et al. 2022. Regionclip: Region-based language-image pretraining. In *Proceedings of the IEEE/CVF Conference on Computer Vision and Pattern Recognition*. 16793–16803.
- [49] Kaiyang Zhou, Jingkang Yang, Chen Change Loy, and Ziwei Liu. 2022. Conditional prompt learning for vision-language models. In *Proceedings of the IEEE/CVF Conference on Computer Vision and Pattern Recognition*. 16816–16825.

- [50] Kaiyang Zhou, Jingkang Yang, Chen Change Loy, and Ziwei Liu. 2022. Learning to prompt for vision-language models. *International Journal of Computer Vision* 130, 9 (2022), 2337–2348.
- [51] Ziqin Zhou, Bowen Zhang, Yinjie Lei, Lingqiao Liu, and Yifan Liu. 2022. ZegCLIP: Towards Adapting CLIP for Zero-shot Semantic Segmentation. *arXiv preprint arXiv:2212.03588* (2022).

A FURTHER ABLATIONS

We ablate the number of resolution scales in our proposed hierarchical patch-text interaction module. The result is summarized in Tab. 5. Specifically, for the 1-Scale interaction (*i.e.*, B4 in Tab. 4), we use a plain ViT [4] with 4 layers and 4 head to maintain similar trainable parameters with our 2-Scale interaction (*i.e.*, B5 in Tab 4). For the 3-Scale interaction, the finest spatial resolution of the feature map is $4p \times 4p$, which is added to the 3rd layer of the density decoder in a similar way as Eqn. 4. We observe that the performance gradually gets better as the number of interactions increases. Using 2-Scale interaction, our method achieves highly competitive results, while more interactions with more parameters no longer lead to significant performance improvement.

Table 5: Ablation on number of scales in hierarchical patch-text interaction module on FSC-147.

Interaction	#Param.	Val MAE	Val RMSE	Test MAE	Test RMSE
1-Scale	16.6M	20.43	69.26	19.26	108.71
2-Scale	17.3M	20.01	66.08	18.77	108.00
3-Scale	24.0M	19.81	66.36	19.00	104.44

B INFERENCE DETAILS

Similar with prior work [19], we apply sliding window during inference time to deal with variable image input size. To be more specific, given an image $I \in \mathbb{R}_{H \times W \times 3}$ we resize it $I' \in \mathbb{R}_{H' \times W' \times 3}$, to make the shortest side becoming 224 pixels while maintaining aspect ratio:

$$\min(H', W') = 224, HW' = H'W \quad (6)$$

Then we apply sliding window algorithm on I' with window size = 224×224 and stride = 128. The predicted density estimation at the overlapped area are averaged.

C ADDITIONAL QUALITATIVE RESULTS

We show more qualitative results on FSC-147, CARPK, and ShanghaiTech Crowd Counting dataset in Fig. 8.

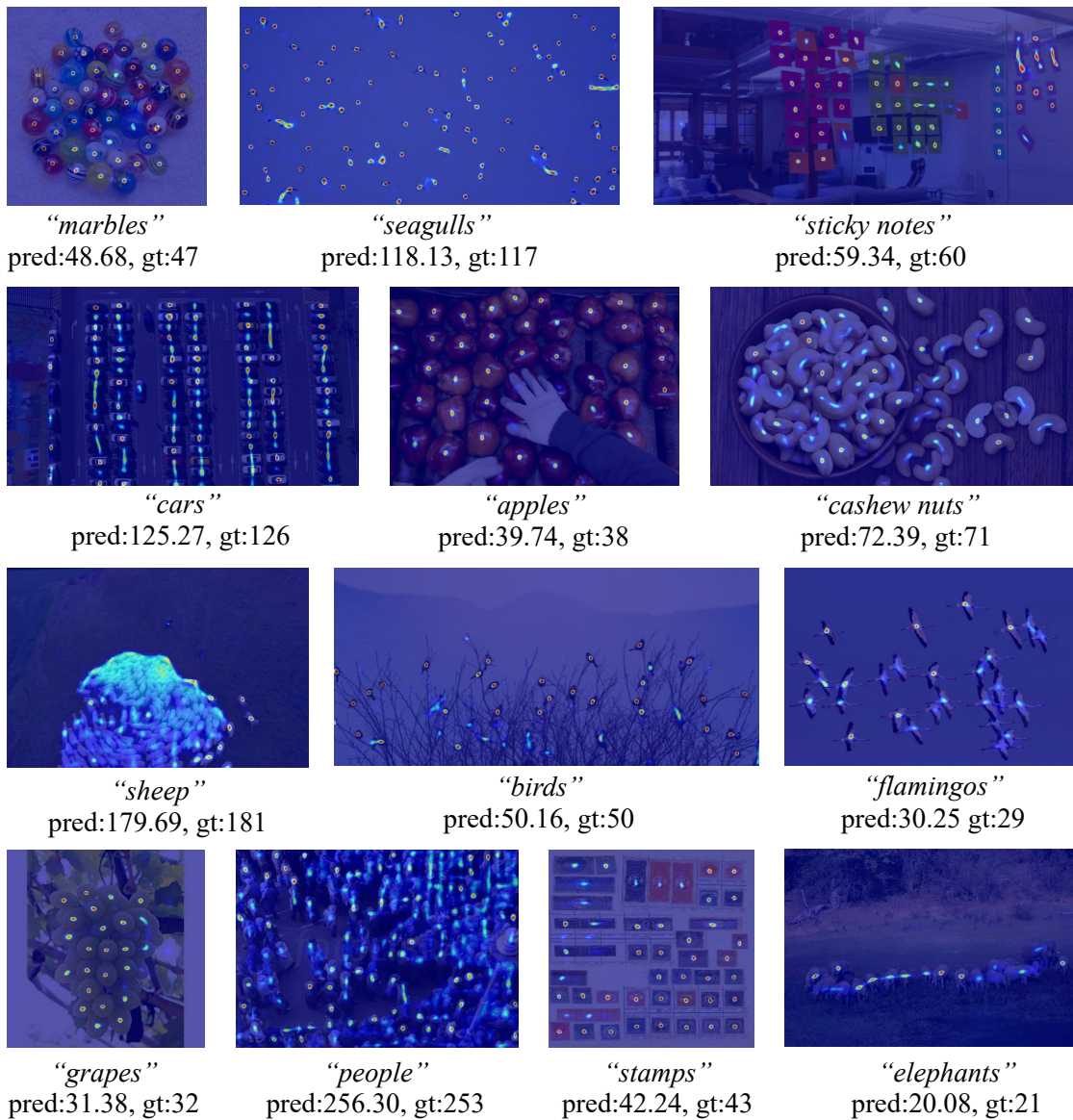


Figure 8: Additional qualitative results. CLIP-Count could generalize well to object with different categories, shapes, sizes, and densities.